metals

MDPI

Article

Enhancing Durability and Resistance to Wear and Corrosion of AISI 431 Martensitic Stainless Steel for Sustainable Engineering Applications

Minerva Rivas-Cabanas, Carolina Camba-Fabal, José Luis Mier-Buenhombre, Laura Castro-Santos, Manuel Ángel Graña-López, Almudena Filgueira-Vizoso and Ana Isabel García-Diez *

Escola Politécnica de Enxeñaría de Ferrol, Centro de Investigacións en Tecnoloxías Navais e Industriais (CITENI), Campus Industrial de Ferrol, Universidade da Coruña, 15403 Ferrol, Spain; minerva.rivas.cabanas@udc.es (M.R.-C.); carolina.camba@udc.es (C.C.-F.); jose.mier@udc.es (J.L.M.-B.); laura.castro.santos@udc.es (L.C.-S.); manuel.grana@udc.es (M.Á.G.-L.); almudena.filgueira.vizoso@udc.es (A.F.-V.)
* Correspondence: ana.gdiez@udc.es

Abstract

This study investigates the influence of heat treatment on the wear resistance and corrosion behavior of AISI 431 martensitic stainless steel, with the aim of enhancing durability and extending service life in demanding applications, thereby supporting more resource-efficient material use. Two single austenitizing treatments (1000 °C and 1070 °C) and one double austenitizing treatment were evaluated. The evolution of hardness, microstructure, wear resistance, and corrosion behavior was determined as a function of the applied heat treatment. Hardness was measured using the Rockwell C method, wear behavior was evaluated by Pin-on-Disk testing, and corrosion resistance was assessed by anodic potentiodynamic polarization tests. The untreated (as-received condition) steel exhibited the lowest wear mass loss. Among the heat-treated samples, the double austenitized condition exhibited the best wear performance. The highest hardness was obtained after single austenitization at 1070 °C (approximately 50 HRC), while double austenitization and single austenitization at 1000 °C resulted in hardness values of approximately 45 HRC. Corrosion testing revealed open-circuit potentials of −0.25 V, −0.27 V, −0.13 V, and −0.14 V for the untreated, SA1000, SA1070, and double-austenitized conditions, respectively. The results show that while SA1070 and DA exhibit more noble open-circuit potentials and extend the stability window against abrupt localized collapse, the DA condition operates under a high-rate non-passive regime with an elevated current density (1.38 mA/cm^2). This thermal treatment shifts the degradation mechanism away from localized intergranular vulnerability at the expense of a higher continuous dissolution rate. Consequently, while DA provides favorable wear behavior among the heat-treated conditions, its elevated current density must be carefully considered for applications in marine environments.

Keywords: AISI 431 martensitic stainless steel; corrosion resistance; wear resistance; heat treatment; durability; resource efficiency; saline environment

Check for updates

Academic Editor: Yanxin Qiao

Received: 16 October 2026
Revised: 14 November 2026
Accepted: 16 November 2026
Published: 18 November 2026

Copyright: © 2026 by the authors. Licensee MDPI, Basel, Switzerland. This article is an open access article distributed under the terms and conditions of the Creative Commons Attribution (CC BY) license.

1. Introduction

Reducing the environmental footprint of engineered systems increasingly requires strategies that go beyond process efficiency and address material demand through material efficiency and circular-economy approaches [1,2]. Material efficiency, understood as providing the same material services with less primary material production, includes strategies

such as lifetime extension, reuse/remanufacturing, and designing with less material, which can reduce upstream energy use and emissions associated with materials production [1]. Recent industrial ecology literature highlights material efficiency as a relevant mitigation lever in climate strategies, complementing supply-side decarbonization of basic materials industries [2,3]. In parallel, the environmental performance of lifetime extension is commonly evaluated within life-cycle assessment (LCA) frameworks, where the way product/service lifetime is defined and modeled can critically influence conclusions about environmental benefits [4].

From a sustainability perspective, extending the service life of engineering components is a direct pathway to improved resource efficiency, as it reduces replacement frequency and the associated material and maintenance demands; such "slowing of resource loops" is central to circular-economy thinking [2,5,6]. This is particularly relevant for systems operating in saline environments, where corrosion and wear limit durability and accelerate life-cycle material consumption; moreover, corrosion has been linked not only to large economic losses but also to a non-negligible carbon footprint associated with replacing degraded steel [6,7]. Accordingly, improving the corrosion and wear resistance of martensitic stainless steels through optimized heat treatment can contribute to both performance and more sustainable material use [1–3]. In this study, single and double austenitizing treatments are assessed in AISI 431 martensitic stainless steel by tracking the evolution of microstructure and hardness and correlating these changes with wear resistance and corrosion behavior.

Martensitic stainless steels are characterized by their high mechanical strength as a result of the heat treatments they undergo (quenching and tempering). However, their corrosion resistance is lower than that of austenitic, ferritic, and duplex stainless steels. The addition of nickel to these steels improves both their mechanical properties and corrosion resistance. This is the case with AISI 431 martensitic stainless steel. This steel is used in marine, aerospace, and chemical industry applications, among others, that meet the aforementioned requirements [7–10]. One of the most promising areas of application for these steels is in the renewable energy sector. Specifically, they are a good option in the manufacture of turbine rotors, both in hydroelectric plants and in wind turbines [11–13].

AISI 431 steel has good mechanical strength and ductility, but its properties are influenced by the manufacturing and processing techniques used, as well as the heat treatments it undergoes [14]. The typical heat treatment for this steel consists of an austenitizing process to dissolve the carbides present in its microstructure, followed by quenching to transform the austenite into martensite (quenching). The steel is then tempered. The resulting microstructure is tempered martensite with undissolved and/or reprecipitated carbides, retained austenite, and delta ferrite. The relative amounts of these microconstituents depend on the specific conditions under which the quenching [15] and subsequent tempering were performed. A high delta ferrite content negatively impacts its mechanical strength, toughness, and corrosion resistance. Additionally, the presence of carbides increases the hardness and strength of martensite after quenching [16]. The tempering temperature is typically between 200 and 300 °C when high mechanical strength and good corrosion resistance are desired, along with moderate toughness. Conversely, if greater toughness is required, the tempering temperature is between 600 and 700 °C, at the expense of reduced mechanical strength and corrosion resistance [17].

The discussion regarding the parameters of the austenitizing process is more complex. Authors such as Ning et al. [18] state that at an austenitizing temperature below 1100 °C, the mechanical strength of the steel will depend primarily on the degree of dissolution of the carbides and alloying elements of the austenite, since the fraction of delta ferrite present during the austenitizing process does not increase. Therefore, the usual

practice is to carry out heating within a temperature range of 950 to 1100 °C. However, other authors [17,19] suggest a narrower range of optimal austenitizing temperatures, placing it between 1050 and 1100 °C. In their work, they state that austenitizing temperatures below 1000 °C do not allow for the dissolution of a large amount of carbides, which has a detrimental effect on the final mechanical strength. On the other hand, they establish that if the temperature exceeds 1100 °C, the dissolution of carbides is permitted, but this results in an increase in the austenite grain size and a higher fraction of retained austenite and delta ferrite.

Replacing single austenitizing with double austenitizing is a technique being used with good results in various steels [20–22]. Authors such as Kahni et al. [23] have established that the finer grain size achieved with double austenitizing can lead to a significant improvement in steel toughness for the same mechanical strength and hardness. Liu et al. [24] reached the same conclusion, also establishing that the yield strength increases as a consequence of the smaller average size of the precipitated carbides. However, Ögel et al. [25] found that the precipitation of fine carbides decreases fracture toughness compared to the same steel subjected to single austenitizing. These authors attribute this effect to the fact that the second austenitizing process, carried out at a lower temperature than the first, decreases the matrix's solubility. The excess alloying elements precipitate as fine carbides. The presence of these particles at the crack head limits the matrix's plastic deformation capacity, leading to a significant decrease in the energy absorbed before crack propagation and, therefore, a reduction in fracture toughness.

The presence of second-phase particles ahead of the crack front limits the amount of plastic deformation in the matrix and, consequently, causes a significant drop in energy absorption before crack propagation.

However, as mentioned earlier, some of the main applications of martensitic stainless steels stem from their good corrosion resistance, making it necessary to consider the influence of heat treatments in this aspect as well. Dalmau et al. [26] reviewed published works on the corrosion and wear of martensitic stainless steels, highlighting the importance of considering all these aspects and the scarcity of references published after 2005.

Choi et al. [27] found that higher austenitizing temperatures resulted in greater resistance to the onset of localized corrosion. This is due to a lower presence of undissolved carbides and retained austenite.

In another study by Rajasekhar et al. [28], the mechanical behavior of martensitic stainless steels subjected to double austenitization was evaluated, and their corrosion resistance was also observed. In this regard, it was found that corrosion resistance is considerably improved with double austenitization.

Corrosion resistance in martensitic stainless steels is strongly influenced by the amount of chromium retained in solid solution and by the precipitation and dissolution behavior of chromium-rich carbides. Previous studies have shown that carbide precipitation may promote local chromium depletion, reducing the stability of the passive film and increasing susceptibility to localized corrosion. Conversely, appropriate heat treatments can modify carbide distribution and chromium availability, thereby improving corrosion performance. Huang et al. [29] explain how chromium-rich carbides affect the chromium available in the matrix and, consequently, the corrosion response of martensitic stainless steels, discussing the influence of austenitization and tempering on carbide kinetics. Furthermore, Kaneko et al. [30], though focusing on austenitic stainless steel, are frequently cited to support the mechanism of local chromium depletion associated with the precipitation of chromium-rich carbides, demonstrating that it promotes chromium-depleted zones in the surrounding matrix that locally compromise protective surface films. In a recent paper, Bösing et al. [31] studied the influence of austenitization on corrosion behavior

using electrochemical measurements, demonstrating that modifications in thermal processing significantly affect the protective surface properties and microstructural evolution of martensitic stainless steels. These findings highlight the importance of understanding how heat-treatment-induced microstructural changes influence anodic dissolution kinetics and breakdown susceptibility. Reilhac et al. [32] examined the relationship between microstructure and corrosion in marine environments, concluding that the marine degradation behavior of martensitic stainless steels does not depend solely on nominal chromium content; rather, it is strongly driven by the phases and heterogeneities developed during thermal processing. Radwan et al. [33] established that pitting and localized breakdown remain primary degradation mechanisms for these steels in chloride-containing media. Additionally, Ocampo et al. [34] linked local chromium depletion to specific treatment parameters, concluding that enhanced corrosion resistance requires a homogeneous distribution of chromium in solid solution, whereas carbide precipitation facilitates localized attack.

Regarding advanced thermal processing, previous studies have demonstrated the beneficial effects of double austenitization on the microstructure, mechanical properties, and anodic stability of martensitic stainless steels. Balan et al. [17] investigated the influence of single and double austenitization on the microstructure and mechanical properties of 16Cr-2Ni steel, highlighting improvements in strength and toughness associated with microstructural modifications. Similarly, Rajasekhar et al. [28] reported an expanded electrochemical stability window and improved mechanical properties in electron beam-welded AISI 431 subjected to double austenitization. However, the combined influence of these heat treatments on the microstructure, hardness, wear behavior, and high-rate dissolution or non-passive response in wrought AISI 431 steel has not been thoroughly assessed. The present work aims to address this issue by establishing correlations between microstructural evolution and the resulting wear and electrochemical response of AISI 431 subjected to single and double austenitization treatments.

In this work, we propose a comparative study of AISI 431 martensitic stainless steel subjected to several heat treatments: single austenitizing at 1000 °C and 1070 °C followed by oil quenching, and double austenitizing (first at 1070 °C and then at 1000 °C) followed by oil quenching. Subsequently, each of the austenitized samples was subjected to a tempering treatment at 550 °C for one hour, followed by air cooling. The objective is to determine which of the three treatments provides the best overall mechanical and corrosion resistance. To achieve this objective, the treated steel was subjected to mechanical, tribological, and electrochemical tests. To determine wear behavior, the ASTM G99-23 standard [35] was followed, while hardness was determined using the Rockwell C test [36]. Finally, corrosion resistance was evaluated using electrochemical tests with anodic potentiodynamic polarization tests performed in 3 wt.% NaCl solution [37]. By identifying a heat treatment that enhances resistance to wear and corrosion in saline environments, this study supports durability-driven approaches to extend service life and improve resource efficiency in metallic components.

2. Materials and Methods

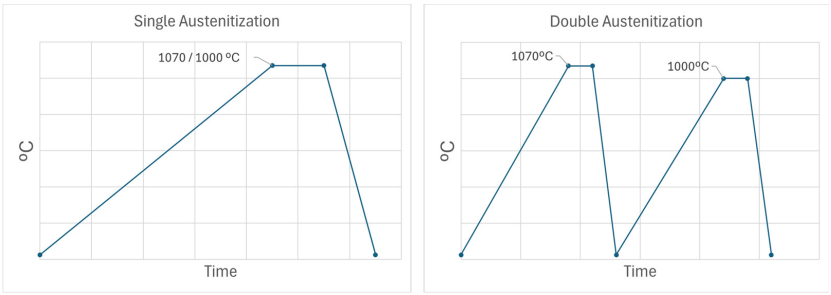
2.1. Materials

To carry out the proposed study, an AISI 431 martensitic stainless steel with the chemical composition shown in Table 1 was used:

Table 1. Chemical composition of AISI 431 martensitic stainless steel. Reprinted from Ref. [38].

C	Si	Mn	P	S	Cr	Ni
0.12–0.22	≤1.00	≤1.50	≤0.040	≤0.015	15.0–17.0	1.50–2.50

Various heat treatments were performed on this material to determine the influence of the austenitizing temperature on its mechanical and tribological properties, as well as its corrosion resistance. These treatments consisted of austenitizing at 1070 °C for 30 min followed by oil quenching (SA1070), and austenitizing at 1000 °C for 30 min followed by oil quenching (SA1000). In addition, the steel was subjected to double austenitizing (DA) to determine whether this treatment improved its performance compared to the previously described treatments. This treatment consisted of austenitizing at 1070 °C for 20 min and oil quenching, followed by a second austenitizing at the lower temperature of 1000 °C for 20 min, also followed by oil quenching. The treatment parameters were selected considering previous work by other authors [15–17,19,23]. Figure 1 illustrates the treatments performed on the steel.



(**a**) (**b**)

Figure 1. Single and double austenitization heat treatments applied to AISI 431 martensitic stainless steel: (**a**) austenitization at 1070 or 1000 °C; (**b**) double austenitization.

Following each of the described treatments, all samples were tempered at 550 °C for one hour and then air-cooled. This temperature is at the lower limit of that determined by Balan et al. [17], aiming to achieve good toughness values without significantly compromising mechanical strength and corrosion resistance. Since the tempering treatment is common to all three austenitizing treatments used, its influence on the final properties will not alter the conclusions drawn.

2.2. Experimental Procedure

The evaluation of the mechanical properties of heat-treated AISI 431 martensitic stainless steel was performed using Rockwell C hardness tests [36] with a Hoytom model 1003 A durometer (HOYTOM, S.L., Leioa, Spain). The test load specified in this standard is 150 kgf. The indentations were distributed across the surface to minimize the influence of potential local microstructural heterogeneities and to obtain representative hardness values for each condition.

To evaluate the tribological behavior, wear tests were carried out using a Pin-on-Disk tribometer (MT-Microtest model MT/30/SCM/T) [35]. A normal load of 20 N and a linear sliding speed of 0.25 m/s were applied, reaching a total sliding distance of 1000 m for each sample. The pin material was a 4 mm tungsten carbide ball with a hardness of 91 HRA. This hardness is significantly higher than that of the steels being tested, which ensured that the primary wear mechanism was abrasion. Since the material being evaluated is always the same, but in different structural states, the comparison of wear behavior between the samples was performed by measuring the mass loss experienced during the test. The mass loss was determined using a Denver Instrument GmbH TB series analytical balance (Denver Instrument, Bohemia, NY, USA) with a precision of 0.00001 g. To avoid the influence of surface finish on the observed results, the samples were previously subjected to a surface preparation process that reduced their roughness (Ra) to values below 0.8 µm. The surface roughness of the samples was determined using a TESA Technology Rugosurf

90G profilometer (TESA Technology, Renens, Switzerland), in accordance with the ISO 4287 standard [39].

Corrosion behavior was studied using anodic potentiodynamic polarization tests performed in a 3 wt.% NaCl solution [37]. The electrochemical tests were performed using an AUTOLAB PGSTAT 204 potentiostat (Metrohm Autolab B.V., Utrecht, The Netherlands) in a conventional three-electrode electrochemical cell with a capacity of 400 mL. The maximum current compliance of the instrument was 400 mA. When this limit was reached, the NOVA software (Metrohm Autolab B.V., Utrecht, The Netherlands, https://www.metrohm-autolab.com/products/software/nova (accessed on 16 October 2026)) automatically restricted the current increase and could terminate the scan to protect the electrochemical system. An Ag/AgCl DJ WOC SGJ reference electrode was employed as the reference electrode throughout the experiments. This method was employed to evaluate the susceptibility to electrochemical breakdown and localized degradation under anodic polarization. E_b was defined as the potential at the intersection of the tangent line drawn along the non-passive plateau and the tangent line representing the rapid increase in current density during transpassive breakdown. In this case, the samples underwent a pre-polishing process similar to that used for metallographic observation. An aqueous solution of 3 wt.% sodium chloride in distilled water was used as the electrolyte. The parameters used in this test were as follows:

- Solution temperature: 20 °C
- Upper potential: 0.7 V vs. OCP
- Lower potential: −0.4 V vs. OCP
- Sweep speed: 0.004 V/s

Although the lower limit defined in the experimental method was −0.4 V vs. OCP, the effective starting potential of the recorded polarization curves depended on the electrochemical stabilization of each specimen and was typically around 0.15 V below the measured OCP.

The metallographic study was performed using a TECMICRO TEC-2000I optical microscope (Tecmicro S.A., Madrid, Spain), complemented by scanning electron microscopy (SEM) using a JEOL JSM-6400 microscope (JEOL Ltd., Akishima, Tokyo, Japan). Prior to the observation stage, the samples were ground, polished with diamond paste, and etched with Kalling I reagent for 10 s [40].

Figure 2 summarizes the experimental procedure carried out in this work.

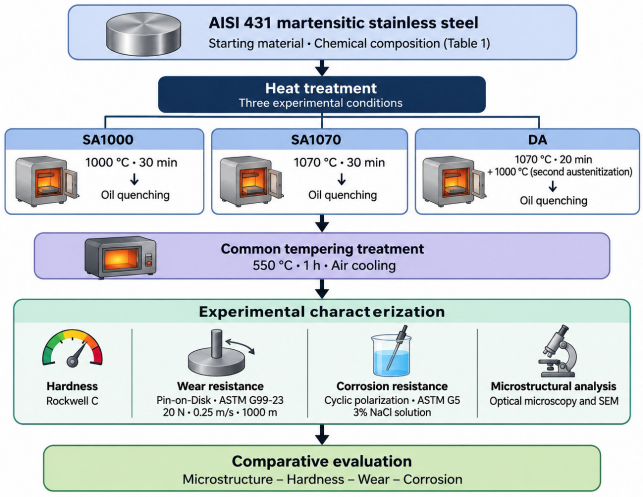


Figure 2. Schematic representation of the experimental workflow followed in this study, including the heat treatment conditions applied to AISI 431 martensitic stainless steel, the subsequent tempering

process, and the mechanical, tribological, electrochemical, and microstructural characterization techniques employed.

3. Results

Figure 3 shows the hardness results obtained for the different treated samples, comparing them with the values of as-cast steel. It can be observed that the hardness value increases significantly with each of the austenitizing treatments evaluated. The results obtained for single austenitizing at a low temperature (1000 °C) are the same as those obtained for double austenitizing. In the case of austenitizing at a high temperature (1070 °C), the hardness value achieved is slightly higher than that of the other two (approximately 5 HRC points higher).

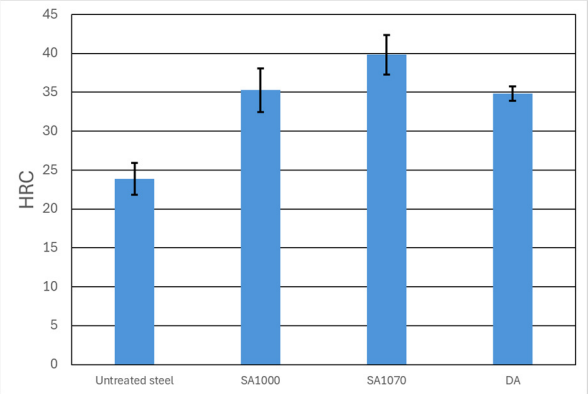


Figure 3. Hardness results obtained for untreated steel and steel subjected to single austenitizing heat treatments at 1000 °C and 1070 °C and double austenitizing (mean hardness values and error bars showing the standard deviation).

The results obtained in the Pin-on-Disk tests are shown below (Figure 4). The graph shows the mass loss experienced during the test for each sample compared to the average coefficient of friction measured throughout the test. In this case, there is also a significant change compared to the untreated steel, which exhibits the best wear resistance. Regarding the results obtained for the heat-treated samples, the best result is achieved with the double austenitizing treatment. This condition exhibits substantially better wear resistance than the low-temperature-austenitized steel (SA1000) and a moderate improvement compared with the high-temperature-austenitized steel (SA1070).

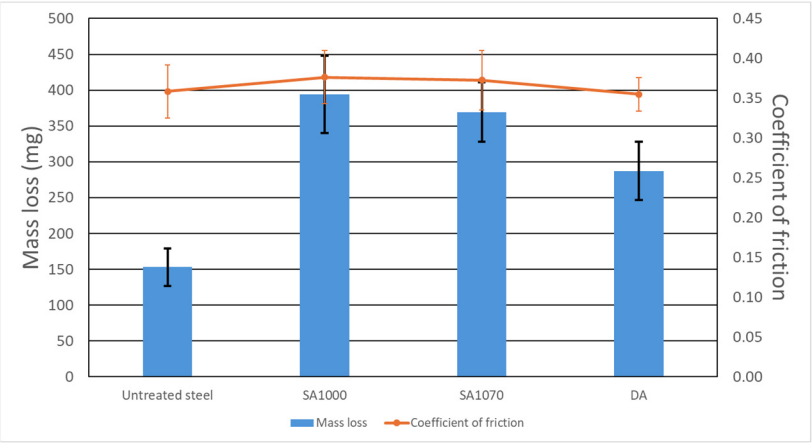


Figure 4. Wear test results: Mass loss and friction coefficient.

The friction coefficient shows a similar pattern, although the variations in it are minimal between samples, with values ranging between 0.355 and 0.376.

Figure 5 shows the polarization curves of the steel subjected to the three heat treatments and of the reference sample of untreated steel, while Table 2 shows the open-circuit potential and breakdown potential values.

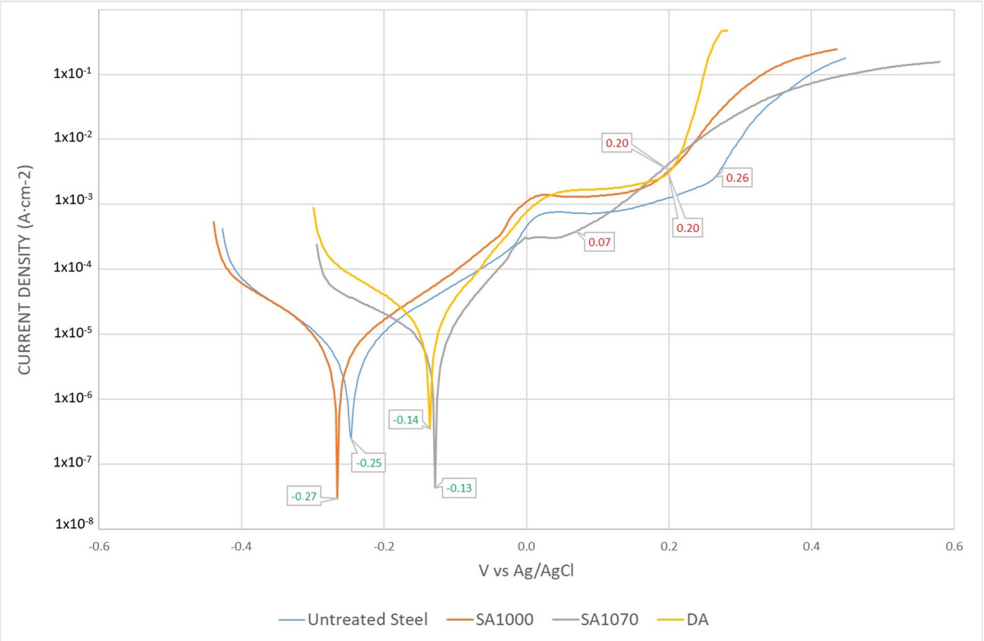


Figure 5. Potentiodynamic polarization curves obtained for the untreated steel, single austenitization at 1000 °C (SA1000), single austenitization at 1070 °C (SA1070), and double austenitization (DA). The values in red correspond to the values for breakdown potential (E_b), and those in green to the values for open-circuit potential (E_{OCP}). The exposed area during the tests was 1 cm^2.

Table 2. Mean open-circuit, breakdown potential values (V vs. Ag/AgCl) and current density obtained in corrosion tests.

	Untreated Steel	SA1000	SA1070	DA
E_{ocp} (V)	−0.25	−0.27	−0.13	−0.14
E_b (V)	0.26	0.20	0.07	0.20
I_{pass} (mA/cm^2)	0.85	1.17	0.40	1.38

The untreated steel and the low-temperature treated steel (SA1000) present more electronegative free corrosion potentials (−0.25 V and −0.27 V). Increasing the temperature to 1070 °C (SA1070) and applying the double treatment (DA) drastically shifts the OCP toward more noble values (−0.13 V and −0.14 V). This demonstrates that raising the austenitization temperature and the double cycle achieves a more effective dissolution of chromium carbides into the matrix, homogenizing the solid solution and making the material thermodynamically more noble.

During the potentiodynamic polarization in 3 wt.% NaCl, all tested conditions exhibit a region where the current density remains relatively stable before increasing abruptly at higher anodic potentials. Although this behavior resembles a stabilization region in the polarization curves, the relatively high current density values recorded in this interval indicate that it cannot be interpreted as a classical passive state. Therefore, the phenomenon is described exclusively in terms of the experimental electrochemical response, without attributing it to any specific surface process or corrosion mechanism. An anodic stabilization

plateau is observed up to approximately 0.26 V for the untreated sample and 0.20 V for the SA1000 sample. Upon reaching these breakdown potentials (E_b) the curves undergo a sharp slope transition toward higher currents, marking the onset of accelerated dissolution triggered by the chloride ions in the medium. In the case of SA1070, immediately following (E_{OCP}), the current rises steeply until reaching an inflection point at 0.07 V, beyond which current growth continues to accelerate, indicating an early breakdown of the transient surface layer compared to the SA1000 sample. For the double-austenitized (DA) sample, a stabilized current plateau is sustained between 0.00 V and 0.20 V. However, despite this extended potential window, the plateau operates at a relatively high current magnitude, characteristic of a non-passive regime rather than a true passive film. Upon reaching 0.20 V, the system undergoes a rapid electrochemical breakdown, where the current increases sharply within a narrow potential interval, representing a severe and rapid acceleration of the dissolution process.

The analysis of the anodic current density values within this stabilization plateau reveals that the SA1070 treatment exhibits the lowest current density at 0.40 mA/cm^2, offering a temporarily lower dissolution rate compared to the untreated steel (0.85 mA/cm^2). However, this region cannot be classified as a truly ideal passive state due to the elevated magnitude of the current densities (in the order of mA/cm^2), which typically indicates non-passive behavior or a diffusion-limited dissolution process driven by the highly aggressive 3 wt.% NaCl environment. Within this context, the lower current value of SA1070 exhibits the lowest current density within the stabilization region of the polarization curve. Although the lower current density of the SA1070 condition indicates a reduced anodic dissolution rate compared with the other heat-treated samples, the underlying mechanism cannot be established from the present results and will require additional surface characterization of the polarized specimens. Conversely, the SA1000 and DA treatments exhibit even higher plateau currents, elevating the current density to 1.17 and 1.38 mA/cm^2, respectively. These results indicate greater anodic activity under the applied polarization conditions. However, the experimental data do not allow identification of the specific microstructural or electrochemical mechanisms responsible for this behavior.

The photomicrographs obtained by optical microscopy can be seen in Figure 6. In the images on the left, the tempering structure of each austenitizing treatment can be observed with a magnification of ×200, while those on the right correspond to the images obtained at 500 magnification.

The untreated steel shows a ferritic matrix and homogeneously distributed carbides in its microstructure. The size of the carbides observed in this case (Figure 6a) is larger than that seen in the other micrographs obtained for the treated steel.

In the case of steel subjected to low-temperature austenitization (SA1000, Figure 6b), carbides appear more frequently in the micrographs than in single high-temperature austenitization (SA1070, Figure 6c), which is consistent with expectations since higher austenitization temperatures increase carbide dissolution capacity. In the first case (SA1000) small amounts of retained austenite are also present, which agrees with the results obtained by Choi et al. [27]. In their study, they found that retained austenite is present when the austenitization temperature is below 1050 °C. This sample exhibits greater microstructural heterogeneity compared to the untreated steel.

When the single austenitizing temperature reaches 1070 °C (SA1070, Figure 6c) the steel exhibits three distinct phases in its microstructure: small amounts of delta ferrite, a matrix of re-martensite, and carbides. The appearance of delta ferrite is common, as established by Mirzaee et al. [19], when the austenitizing temperature exceeds 1050 °C.

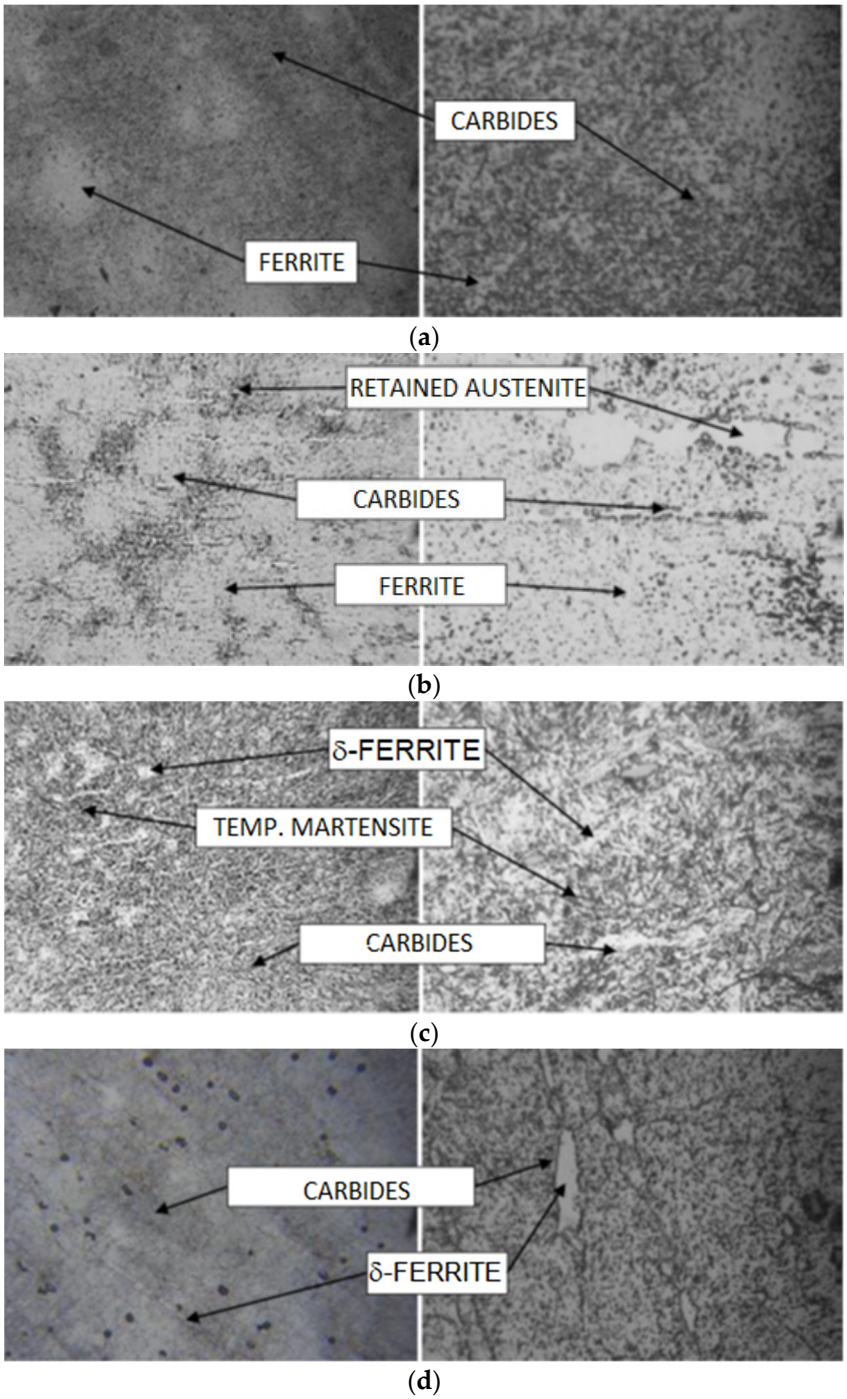


Figure 6. Results of the metallographic analysis performed by optical microscopy: (**a**) untreated steel; (**b**) steel subjected to single austenitization at 1000 °C; (**c**) steel subjected to single austenization at 1070 °C; (**d**) steel subjected to double austenitization.

Finally, Figure 6d shows the microstructure present in the steel subjected to double austenitization (DA), where a greater amount of delta ferrite can be observed than in the SA1070 treatment. The appearance of precipitated carbides at the grain boundaries appears less evident than in the other samples.

Metallographic analysis using optical microscopy was complemented by scanning electron microscopy (SEM) coupled with energy-dispersive X-ray spectroscopy (EDS). Figure 7 shows the micrographs obtained for the untreated steel, where a chromium-rich region is observed, which is likely associated with carbide.

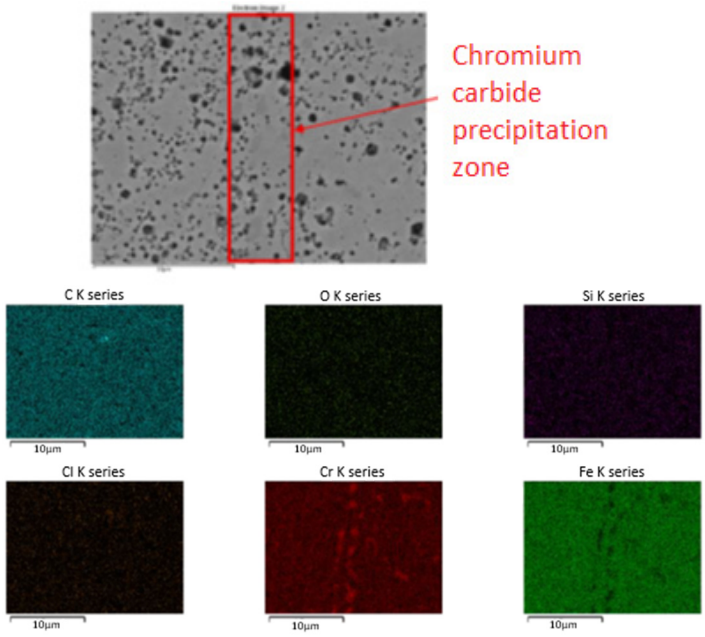


Figure 7. SEM/EDS results of untreated steel.

Figure 8 shows the results obtained for the sample subjected to single austenitization at 1000 °C. In this case, areas with higher oxygen concentrations can be observed. Areas with higher chromium concentrations and decreased oxygen and iron concentrations were also observed, which, as in the previous case, could indicate the presence of chromium carbides. This behavior may be associated with the comparatively low austenitizing temperature (1000 °C), which may have led to incomplete dissolution of chromium carbides prior to quenching, promoting the persistence of chromium-rich regions within the microstructure.

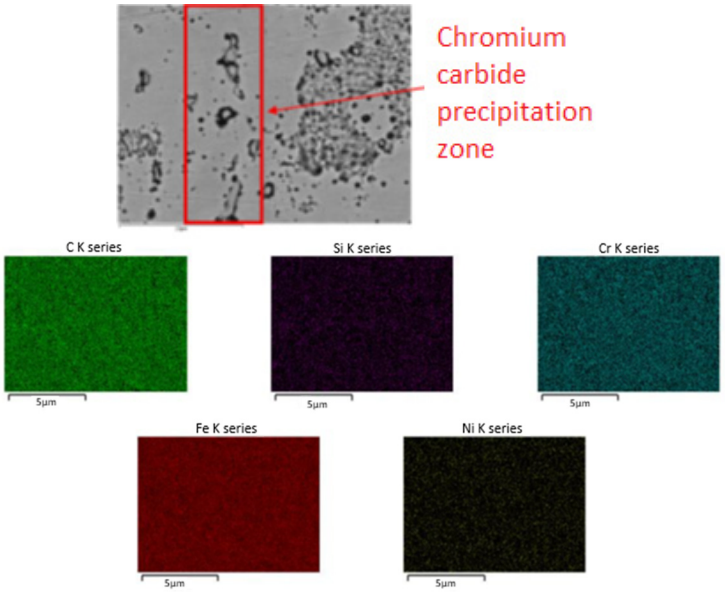


Figure 8. SEM/EDS results of steel subjected to austenitization at 1000 °C.

When the austenitizing temperature is increased (Figure 9) the distribution of chromium is more homogeneous, which is consistent with the greater dissolving capacity of chromium at higher temperatures.

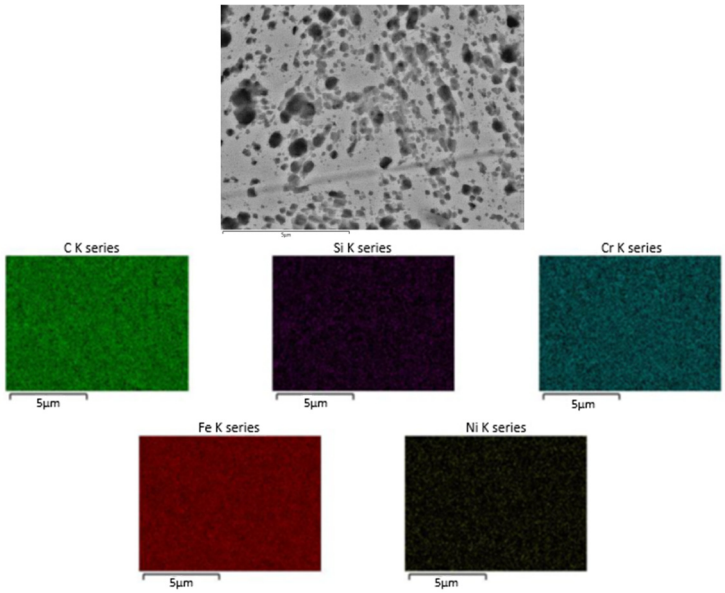


Figure 9. SEM/EDS results of steel subjected to austenitization at 1070 °C.

Finally, double-austenitized steel exhibits a more uniform distribution of its constituent elements (Figure 10).

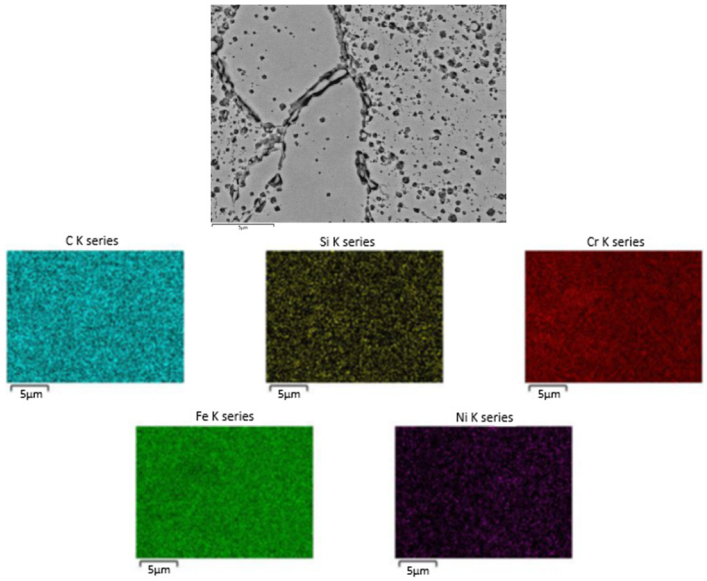


Figure 10. SEM/EDS result of steel subjected to double austenitization.

4. Discussion

Figure 11 shows a comparison of the hardness and mass loss results obtained in the Pin-on-Disk wear test for the different treated steels and for the untreated steel used as a reference. The results reveal that the relationship between hardness and wear resistance is not straightforward. While all heat-treated conditions exhibit higher hardness than the untreated steel, they also experience higher mass losses during wear testing. This behavior suggests that wear performance is controlled by a combination of factors, including matrix hardness, carbide content, and carbide distribution within the microstructure.

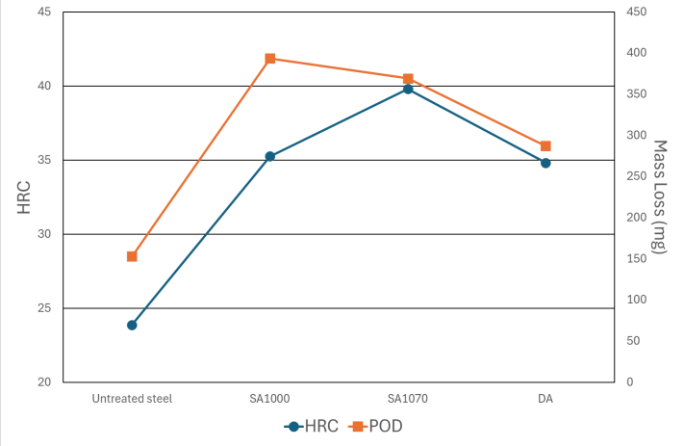


Figure 11. Comparison of hardness and mass loss results in the POD wear test of the different samples.

As discussed in the previous section, the steel with the lowest hardness is the untreated steel, which has a ferritic matrix and a lower carbide content than the other steels evaluated (Figure 6). The remaining steels have harder matrices (delta ferrite or tempered martensite) and a higher carbide content, which contributes to their increased hardness. The highest hardness value is observed for the steel austenitized at 1070 °C, which exhibits a predominantly tempered martensitic matrix together with finely distributed carbides.

The greater mass loss during the wear test of the heat-treated samples may be associated with the detachment of the hardest particles (precipitated carbides) from the matrix. This phenomenon could explain why materials with greater hardness exhibit lower wear resistance, which depends on several factors: the quantity, size, and distribution of the carbides, and the relative hardness between the matrix and the abrasive particles [41–43]. The detachment of these hard particles could produce an abrasive effect during the test, leading to greater mass loss. A similar mechanism may also explain the changes in the coefficient of friction measured during the wear tests (Figure 4), where an increase in the measured value can be observed for the samples subjected to single austenitization. This could be attributed to increased abrasion resulting from the presence of hard particles detached from the matrix.

Thus, double-austenitized steel, which has a hardness similar to that austenitized at 1000 °C and lower than that at 1070 °C, exhibits better wear resistance. This behavior may be related to the combination of a harder matrix than that of the steel treated at 1000 °C, a lower amount of precipitated carbides than that observed in the steel treated at 1070 °C, and a more homogeneous microstructure than those of the other two heat-treated conditions. Similarly, the lower wear resistance observed in the low-temperature-austenitized steel may be associated with its carbide distribution, carbide content, and comparatively softer matrix.

A possible explanation for the greater wear resistance observed in the untreated steel is the more homogeneous distribution and larger size of the carbides present in the microstructure. Such characteristics may reduce the tendency for particle detachment and consequently decrease the likelihood of wear processes involving loose abrasive particles. However, additional characterization of wear tracks and wear debris would be required to confirm this hypothesis.

Literature widely supports that heat treatment at high austenitization temperatures (typically > 1050 °C) causes the complete dissolution of complex chromium carbides (such as Cr23C6) into the austenite or ferrite matrix [44]. In untreated samples or those treated at low temperatures (SA1000), the precipitation of these carbides generates adjacent chromium-depleted zones (sensitization phenomenon) [45]. Upon carbide dissolution at 1070 °C, chromium homogenizes within the solid solution, increasing the overall thermodynamic

resistance of the matrix and causing the open-circuit potential (E_{OCP}) to shift toward more noble values.

The comparative analysis between the double austenitization (DA) treatment and the untreated steel highlights how the thermal modification alters the underlying corrosion mechanisms of the base material. In high-chromium martensitic stainless steels, the untreated state is highly susceptible to sensitization [46] where an unhomogenized microstructure promotes the precipitation of chromium-rich carbides along the grain boundaries, leaving adjacent zones severely depleted of chromium. This phenomenon could explain the significantly electronegative open-circuit potential of the untreated steel (−0.25 V), indicating a thermodynamically active and localized vulnerability. Although the untreated sample displays a high breakdown potential (0.26 V), this apparent resistance is deceptively favorable; due to its lower (E_{OCP}), the material experiences a broad stabilization region during anodic polarization, associated with a current density of approximately 0.85 mA/cm^2. The DA treatment successfully shifts the system away from this severe intergranular vulnerability by homogenizing the microstructure. However, the subsequent elevation of the plateau current density to 1.38 mA/cm^2 under polarization indicates that while localized sensitization effects may be mitigated, the resulting surface layer transitions into a high-rate non-passive dissolution state regulated by mass-transport limitations in the chloride-rich medium.

Therefore, the double austenitizing treatment provides the best wear performance among the heat-treated conditions and exhibits a more noble open-circuit potential than both the untreated steel and the SA1000 condition. However, its high non-passive current density indicates an increased dissolution rate under anodic polarization. Consequently, the DA treatment should be regarded as a compromise between wear performance and electrochemical behavior rather than as a condition with the highest overall corrosion resistance.

5. Conclusions

This study evaluated the wear and corrosion resistance of AISI 431 martensitic stainless steel subjected to different heat treatments, with the aim of determining the option that offers the best performance in highly saline environments, such as offshore wind farms or similar coastal installations. The conclusions obtained are as follows:

- The hardness of AISI 431 steel increases with the austenitizing temperature. This behavior is likely associated with the microstructural changes induced by the higher austenitizing temperature, which result in a more homogeneous microstructure predominantly composed of tempered martensite.
- Double austenitizing leads to a hardness similar to that of low-temperature austenitizing.
- Greater hardness does not necessarily imply better wear resistance. The lower wear resistance observed in the heat-treated steels may be associated with the detachment of hard particles from the microstructure and the resulting abrasive interactions during sliding. This effect appears to be more pronounced in the low-temperature-austenitized steel, which exhibits a higher carbide population and a softer matrix than the other heat-treated conditions.
- Of the three heat treatments evaluated, double austenitization provides the best wear performance. This behavior may be related to the combination of a harder matrix than that of the SA1000 condition, a lower carbide content than that observed in the SA1070 condition, and a more homogeneous microstructure.
- Although increasing the austenitization temperature to 1070 °C (SA1070) promotes the dissolution of chromium carbides and shifts the (E_{OCP}) to a more noble value (−0.13 V), the resulting surface layer exhibits low stability under polarization. This

is evidenced by a premature breakdown and a steady acceleration of the dissolution current starting at potentials as low as 0.07 V.

- The double austenitization (DA) treatment provides a distinct trade-off between thermodynamic nobility and polarization stability. While it successfully offsets the premature breakdown potential observed in the single SA1070 treatment (extending the stabilization window up to 0.20 V) it records the highest plateau current density (1.38 mA/cm^2). This elevated value indicates an accelerated anodic dissolution rate during polarization compared with the other investigated conditions. However, additional surface characterization will be required to determine the mechanisms responsible for this behavior.
- Conversely, while the untreated steel and SA1000 samples display more electronegative open-circuit potentials, they exhibit a lower steady-state dissolution rate within their stabilization regions, delaying the final transpassive or localized breakdown up to 0.26 V and 0.20 V, respectively. This indicates greater stability of the electrochemical response prior to breakdown in the untreated and SA1000 conditions compared to the DA-treated sample in the chloride-rich medium.

Among the heat-treated conditions evaluated, the double-austenitized steel exhibited the most favorable wear performance. Although it cannot be considered the condition with the highest overall corrosion resistance, it displayed a more noble open-circuit potential than the untreated steel and the SA1000 condition, indicating improved thermodynamic stability. This is particularly relevant for components intended to operate in saline or chloride-containing environments, where corrosion resistance becomes a critical factor governing long-term service performance. Therefore, among the three heat-treated conditions investigated (DA, SA1000 and SA1070), double austenitization appears to be the most suitable treatment when wear performance is prioritized while maintaining a comparatively noble electrochemical response in this medium.

From a durability and life-cycle perspective, improving resistance to the dominant degradation mechanisms in saline service conditions can extend component service life and reduce replacement frequency, supporting more resource-efficient material use and potentially lowering the environmental footprint associated with maintenance and material consumption.

Author Contributions: Conceptualization, C.C.-F., J.L.M.-B. and A.I.G.-D.; Data curation, M.R.-C., A.F.-V., L.C.-S. and M.Á.G.-L.; Formal analysis, M.R.-C., A.F.-V., L.C.-S. and M.Á.G.-L.; Methodology, C.C.-F. and J.L.M.-B.; Supervision, A.F.-V., L.C.-S. and M.Á.G.-L.; Validation, A.I.G.-D.; Writing—original draft, M.R.-C. and A.I.G.-D.; Writing—review and editing, C.C.-F., J.L.M.-B. and A.I.G.-D. All authors have read and agreed to the published version of the manuscript.

Funding: This research was supported by the "Aid for the consolidation and structuring of competitive research units", Xunta de Galicia. Reference number: ED431B/2025/39.

Data Availability Statement: The original contributions presented in this study are included in the article. Further inquiries can be directed to the corresponding author.

Conflicts of Interest: The authors declare no conflicts of interest.

References

1. Allwood, J.M.; Ashby, M.F.; Gutowski, T.G.; Worrell, E. Material Efficiency: A White Paper. *Resour. Conserv. Recycl.* **2011**, *55*, 362–381. [CrossRef]
2. Bocken, N.M.P.; de Pauw, I.; Bakker, C.; van der Grinten, B. Product Design and Business Model Strategies for a Circular Economy. *J. Ind. Prod. Eng.* **2016**, *33*, 308–320. [CrossRef]
3. Masanet, E.; Heeren, N.; Kagawa, S.; Cullen, J.; Lifset, R.; Wood, R. Material Efficiency for Climate Change Mitigation. *J. Ind. Ecol.* **2021**, *25*, 254–259. [CrossRef]

4. Jerome, A.; Ljunggren, M. Product Lifetime in Life Cycle Assessments of Circular Economy Strategies—A Review and Consolidation of Methodology. *Int. J. Life Cycle Assess.* **2025**, *30*, 2162–2189. [CrossRef]
5. Mesa, J.A.; Gonzalez-Quiroga, A.; Aguiar, M.F.; Jugend, D. Linking Product Design and Durability: A Review and Research Agenda. *Heliyon* **2022**, *8*, e10734. [CrossRef] [PubMed]
6. Iannuzzi, M.; Frankel, G.S. The Carbon Footprint of Steel Corrosion. *npj Mater. Degrad.* **2022**, *6*, 101. [CrossRef] [PubMed]
7. Lo, K.H.; Shek, C.H.; Lai, J.K.L. Recent Developments in Stainless Steels. *Mater. Sci. Eng. R Rep.* **2009**, *65*, 39–104. [CrossRef]
8. Barbosa, C.; Abud, I. Recent Developments on Martensitic Stainless Steels for Oil and Gas Production. *Recent Pat. Corros. Sci.* **2013**, *3*, 27–38. [CrossRef]
9. Andersson, R.; Schedin, E.; Magnusson, C.; Ocklund, J.; Persson, A. *The Applicability of Stainless Steel for Crash Absorbing Components*; SAE Technical Papers; SAE International: Warrendale, PA, USA, 2002. [CrossRef]
10. Saha Podder, A.; Bhanja, A. Applications of Stainless Steel in Automobile Industry. *Adv. Mat. Res.* **2013**, *794*, 731–740. [CrossRef]
11. Berbecaru, A.C.; Coman, G.; Gradinaru, C.S.; Sohaciu, M.G.; Predescu, C.; Dumitrescu, R.E.; Ciuca, S.; Gherghescu, I.A. Microstructural Characterization of Some Turbine Blade Martensitic Stainless Steels. *Rev. De Chim.* **2019**, *70*, 1132–1139. [CrossRef]
12. Sathish, S.; Beena, T.; Rahul, V.; Kumar, M.S.; Das, A.D.; Seema, B.; Ram, R. Assessment of Wear Behavior Analysis on Normalized Martensitic Stainless Steel for Sustainable Applications. In *Proceedings of the E3S Web of Conferences*; EDP Sciences: Les Ulis, France, 2024; Volume 552.
13. Coman, G.; Cristian Pantilimon, M.; Gabriela Sohaciu, M.; Ciucă, S.; Constantin Berbecaru, A.; Cristian Pantilimon, M.; Gabriela Sohaciu, M.; Grădinaru, C.; Predescu, C. New Martensitic Stainless Steel Hardenable by Precipitation for Hydropower Turbines. *U.P.B. Bull. Ser. B* **2017**, *79*, 210–218.
14. Liu, Y.; Li, A.; Cheng, X.; Zhang, S.Q.; Wang, H.M. Effects of Heat Treatment on Microstructure and Tensile Properties of Laser Melting Deposited AISI 431 Martensitic Stainless Steel. *Mater. Sci. Eng. A* **2016**, *666*, 27–33. [CrossRef]
15. Vivas, J.; Capdevila, C.; Altstadt, E.; Houska, M.; San-Martín, D. Importance of Austenitization Temperature and Ausforming on Creep Strength in 9Cr Ferritic/Martensitic Steel. *Scr. Mater.* **2018**, *153*, 14–18. [CrossRef]
16. Rajasekhar, A.; Madhusudhan Reddy, G.; Mohandas, T.; Murti, V.S.R. Influence of Austenitizing Temperature on Microstructure and Mechanical Properties of AISI 431 Martensitic Stainless Steel Electron Beam Welds. *Mater. Des.* **2009**, *30*, 1612–1624. [CrossRef]
17. Balan, K.P.; Venugopal Reddy, A.; Sarma, D.S. Effect of Single and Double Austenitization Treatments on the Microstructure and Mechanical Properties of 16Cr-2Ni Steel. *J. Mater. Eng. Perform.* **1999**, *8*, 385–393. [CrossRef]
18. Ning, L.; Zhonggang, D.; Menggen, H. Effect of Heat Treatment on Microstructure and Mechanical Properties of Martensitic–Ferritic Stainless Steel Containing 17%Cr and 2%Ni. *Mater. Sci. Technol.* **1991**, *7*, 1057–1062. [CrossRef]
19. Mirzaee, M.; Momeni, A.; Aieni, N.; Keshmiri, H. Effect of Quenching and Tempering on Microstructure and Mechanical Properties of 410 and 410 Ni Martensitic Stainless Steels. *J. Mater. Res.* **2017**, *32*, 687–696. [CrossRef]
20. Salunkhe, S.; Fabijanic, D.; Nayak, J.; Hodgson, P. Effect of Single and Double Austenitization Treatments on the Microstructure and Hardness of AISI D2 Tool Steel. *Mater. Today Proc.* **2015**, *2*, 1901–1906. [CrossRef]
21. Ali, M.; Porter, D.; Kömi, J.; Eissa, M.; El Faramawy, H.; Mattar, T. The Effect of Double Austenitization and Quenching on the Microstructure and Mechanical Properties of CrNiMoWMnV Ultrahigh-Strength Steels after Low-Temperature Tempering. *Mater. Sci. Eng. A* **2019**, *763*, 138169. [CrossRef]
22. Li, Z.X.; Tong, B.Q.; Zhang, Q.L.; Yao, J.H.; Kovalenko, V. Microstructure Refinement and Properties of 1.0C-1.5Cr Steel in a Duplex Treatment Combining Double Quenching and Laser Surface Quenching. *Mater. Sci. Eng. A* **2020**, *776*, 138994. [CrossRef]
23. Khani Sanij, M.H.; Ghasemi Banadkouki, S.S.; Mashreghi, A.R.; Moshrefifar, M. The Effect of Single and Double Quenching and Tempering Heat Treatments on the Microstructure and Mechanical Properties of AISI 4140 Steel. *Mater. Des.* **2012**, *42*, 339–346. [CrossRef]
24. Liu, J.; Yu, H.; Zhou, T.; Song, C.; Zhang, K. Effect of Double Quenching and Tempering Heat Treatment on the Microstructure and Mechanical Properties of a Novel 5Cr Steel Processed by Electro-Slag Casting. *Mater. Sci. Eng. A* **2014**, *619*, 212–220. [CrossRef]
25. Ögel, B.; Tekin, E. The Effect of Double Austenitization on the Microstructure and Toughness of AISI M2 High Speed Steel. *Steel Res.* **1998**, *69*, 247–252. [CrossRef]
26. Dalmau, A.; Richard, C.; Igual–Muñoz, A. Degradation Mechanisms in Martensitic Stainless Steels: Wear, Corrosion and Tribocorrosion Appraisal. *Tribol. Int.* **2018**, *121*, 167–179. [CrossRef]
27. Choi, Y.S.; Kim, J.G.; Park, Y.S.; Park, J.Y. Austenitizing Treatment Influence on the Electrochemical Corrosion Behavior of 0.3C–14Cr–3Mo Martensitic Stainless Steel. *Mater. Lett.* **2007**, *61*, 244–247. [CrossRef]
28. Rajasekhar, A.; Madhusudhan Reddy, G. The Effect of Single and Double Austenitization Temperatures on the Microstructure, Mechanical Properties, and Pitting Corrosion of AISI 431 Electron Beam Welds. *Proc. Inst. Mech. Eng. Part L J. Mater. Des. Appl.* **2010**, *224*, 9–18. [CrossRef]
29. Huang, Q.; Volkova, O.; Biermann, H.; Mola, J. Communication Dilatometry Analysis of Dissolution of Cr-Rich Carbides in Martensitic Stainless Steels. *Metall. Mater. Trans. A* **2017**, *48*, 5771–5777. [CrossRef]

30. Kaneko, K.; Fukunaga, T.; Yamada, K.; Nakada, N.; Kikuchi, M.; Saghi, Z.; Barnard, J.S.; Midgley, P.A. Formation of M23C6-Type Precipitates and Chromium-Depleted Zones in Austenite Stainless Steel. *Scr. Mater.* **2011**, *65*, 509–512. [CrossRef]
31. Bösing, I.; Cramer, L.; Steinbacher, M.; Zoch, H.W.; Thöming, J.; Baune, M. Influence of Heat Treatment on the Microstructure and Corrosion Resistance of Martensitic Stainless Steel. *AIP Adv.* **2019**, *9*, 065317. [CrossRef]
32. Reilhac, P.; Creus, J.; Feaugas, X.; Michel, G.; Frappart, S.; Branger, V. Relationship Between Microstructure and Marine Corrosion Resistance of Martensitic Stainless Steels: A Multiscale Approach. *J. Mater. Eng. Perform.* **2019**, *28*, 3785–3802. [CrossRef]
33. Radwan, A.B.; Moussa, A.M.; Al-Qahtani, N.H.; Case, R.; Castaneda, H.; Abdullah, A.M.; El-Haddad, M.A.M.; Bhadra, J.; Al-Thani, N.J. Evaluation of the Pitting Corrosion of Modified Martensitic Stainless Steel in CO_2 Environment Using Point Defect Model. *Metals* **2022**, *12*, 233. [CrossRef]
34. Evia Ocampo, A.; Roßberg, S.; Rohr, J.; Rosemann, P. Effect of Heat Treatment Parameters on Microstructure, Hardness, and Corrosion Resistance of Martensitic Stainless Steel X30Cr13 (AISI 420B). *Mater. Corros.* **2026**, *77*, 1094–1105. [CrossRef]
35. *ASTM G99-23*; Standard Test Method for Wear Testing with a Pin-on-Disk Apparatus. ASTM International: West Conshohocken, PA, USA, 2023.
36. *UNE-EN ISO 6508-1:2024*; Metallic Materials—Rockwell Hardness Test—Part 1: Test Method. International Organization for Standardization: Geneva, Switzerland, 2024.
37. *ASTM G5-94(2011)E1*; Reference Test Method for Making Potentiodynamic Anodic Polarization Measurements. ASTM International: West Conshohocken, PA, USA, 2011.
38. *UNE-EN 10088-1*; Stainless Steels. Part 1: List of Stainless Steels. AENOR: Madrid, Spain, 2024.
39. *UNE-EN ISO 4287:1999/AC:2010*; Geometrical Product Specifications (GPS)—Surface Texture: Profile Method—Terms, Definitions and Surface Texture Parameters. International Organization for Standardization: Geneva, Switzerland, 2010.
40. Hemmati, I.; Ocelík, V.; De Hosson, J.T.M. The Effect of Cladding Speed on Phase Constitution and Properties of AISI 431 Stainless Steel Laser Deposited Coatings. *Surf. Coat. Technol.* **2011**, *205*, 5235–5239. [CrossRef]
41. Chotěborský, R.; Hrabě, P.; Müller, M.; Válek, R.; Savková, J.; Jirka, M. Effect of Carbide Size in Hardfacing on Abrasive Wear. *Res. Agric. Eng.* **2009**, *55*, 149–158. [CrossRef]
42. Pawar, S.; Jha, A.K.; Mukhopadhyay, G. Effect of Different Carbides on the Wear Resistance of Fe-Based Hardfacing Alloys. *Int. J. Refract. Met. Hard Mater.* **2019**, *78*, 288–295. [CrossRef]
43. Van Acker, K.; Vanhoyweghen, D.; Persoons, R.; Vangrunderbeek, J. Influence of Tungsten Carbide Particle Size and Distribution on the Wear Resistance of Laser Clad WC/Ni Coatings. *Wear* **2005**, *258*, 194–202. [CrossRef]
44. Ma, T.; Fu, B.; Guan, W.; Guo, Y.; Fu, L.; Shan, A. Dissolution Behavior of Carbide in 4Cr13 Martensitic Stainless Steel during Austenitizing. *J. Mater. Eng. Perform.* **2024**, *34*, 5394–5401. [CrossRef]
45. da Fonseca, G.S.; Hamberger Ferreira, K.; Carreiro de Oliveira, S.; Sousa Nilo Mendes, P.; da Silva Vitorino, L.P.; Alves Ferreira, E. Influence of Austenitizing, Quenching, and Tempering on the Hardness and Corrosion Resistance in Martensitic Stainless Steel EN 1.4116. *J. Mater. Res. Technol.* **2025**, *36*, 5396–5405. [CrossRef]
46. Rajasekhar, A. Corrosion Behavior of Martensitic Stainless Steels-Role of Composition and Heat Treatment Procedures. *Int. J. Sci. Res. (IJSR)* **2013**, *4*, 2319–7064.

Disclaimer/Publisher's Note: The statements, opinions and data contained in all publications are solely those of the individual author(s) and contributor(s) and not of MDPI and/or the editor(s). MDPI and/or the editor(s) disclaim responsibility for any injury to people or property resulting from any ideas, methods, instructions or products referred to in the content.